Implantable Semi-Active UHF RFID Tag with Inductive Wireless Power Transfer

Jan Kracek, *Member, IEEE*, Milan Svanda, Milos Mazanek, *Senior Member, IEEE*,
Jan Machac, *Senior Member, IEEE*

***Abstract*—The objective of this paper was to design a compact, battery-less system for an implantable semi-active UHF RFID tag with inductive wireless power transfer for the human body. An RFID chip of the tag, combining powering from a reader by communication and from another source through inductive wireless power transfer, was used. Tag sensitivity for communication was increased by about 21 dB with the help of wireless inductive powering when compared to tags which did not employ this system. Communication and powering circuits were integrated within compact structures on the sides of the reader and the tag. The structure for communication and powering on the side of the reader consists of a centre-excised Archimedes spiral antenna and a circular loop respectively. Similarly, the structure on the side of the tag consists of a folded dipole antenna for communication and a rectangular loop for powering.**

***Index Terms*—semi-active RFID, inductive wireless power transfer.**

I. Introduction

Highly integrated low-power chips using radio frequency identification (RFID) enabled the development of implants for monitoring and controlling functions of the human body [1]. This method monitors any object wirelessly at frequencies from tens of kHz up to several GHz for read distances ranging from several millimeters up to a few tens of meters [2]. The monitored object usually has a passive circuitry (RFID tag with chip) which uses power received by communication from a monitoring device (RFID reader).

The semi-active RFID chip can combine powering by the reader and powering by other source. This source can deliver power e.g. by inductive wireless power transfer (IWPT). The IWPT represents an effective method for delivering power wirelessly from a source to an appliance [3]. This method uses frequencies from tens of kHz up to several MHz for delivering power to an appliance from distances of several millimeters up to several meters at an efficiency ranging from several percentage points up to tens of percentage points. Overall performance is deemed to be satisfactory even if the reference levels for electromagnetic field are respected.

The same frequency is usually applied to both communication and powering [1], though a concept with two different frequencies for communication and powering was discussed in [4]. However, the implant described in [4] contains a battery. A concept using three frequencies for forward and backward communication, and powering was proposed in [5], but the implant featured in this concept requires a three-dimensional structure.

The RFID in the UHF frequency band enables the use of antennas of acceptable size for implants [6-8]. However, the considerable dissipation of communication signal power in the human body substantially decreases the read range. This must be compensated by an increase in the transmitted power of the reader. The solution of this problem was presented in [9, 10], using a semi-active RFID chip powered by non-electric sources.

This paper combines a communication scheme based on RFID and a powering scheme based on IWPT for an implantable battery-less tag for humans. The originally proposed two-frequency solution integrates both communication and powering elements into a single structure with communication running at a frequency of 866 MHz (the European UHF frequency band). Powering of the semi-active RFID chip uses IWPT at frequency 6.78 MHz (industrial, scientific and medical frequency band) which assures a low dissipation of power transmitted through the tissue of the human body. The design is compact with a tag size suitable for implantation into the human body and communication sensitivity is increased by 21 dB when the powering is on.

II. System Design

The geometry of the arrangement and the scheme of the reader and tag sides are shown in Fig. 1 and Fig. 2 respectively. Communication and powering circuits are integrated into compact structures on the respective sides of the reader and the tag. A structure on the side of the reader for communication and powering consists of a centre-excised Archimedes spiral antenna and a circular loop respectively, as seen in Fig. 3. Similarly, a structure on the side of the tag consists of a folded dipole antenna and a rectangular loop, as

Manuscript received October, 2015; accepted January, 2016. Date of publication xx. This work has received support from Ministry of Education Youth and Sports under project LD14122 Electromagnetic Structures and Circuits for Wireless Power Transmission, which is related to project ICT COST Action IC1301 Wireless Power Transmission for Sustainable Electronics (WiPE). The authors wish to thank the ASICentrum spol. s r.o. company for supplying RFID chip samples for the experiment.

The authors are with the Department of Electromagnetic Field, Faculty of Electrical Engineering, Czech Technical University in Prague, Technicka 2, 166 27 Prague, Czech Republic (e-mail of the corresponding author: svanda.milan@fel.cvut.cz).

Digital Object Identifier inserted by IEEE.

shown in Fig. 4. The structures are realized on a Taconic RF 30 substrate (ε_r = 3.00, tan(δ) = 0.0014, h = 0.76 mm). Additional circuitries are connected between the powering pins of the RFID chip of the tag and the rectangular loop, or, to the circular loop to assure efficient powering by IWPT. Parameters of the RFID reader and chip are presented in datasheets [11, 12].

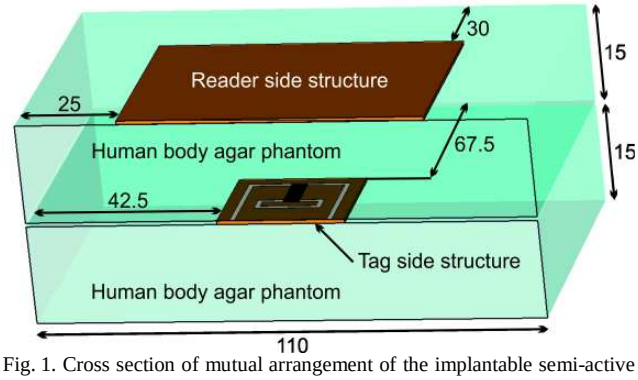

Fig. 1. Cross section of mutual arrangement of the implantable semi-active UHF RFID tag with IWPT in a human body agar phantom and the reader side structure lying on the surface of the phantom (dimensions in mm). Tag side structure is centered in the middle of the phantom.

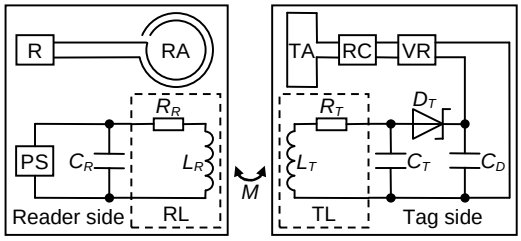

Fig. 2. Scheme of the system (R – Reader, RA – Reader Antenna, TA – Tag Antenna, RC – RFID Chip, VR – Voltage Regulator, PS – Power Source, RL – Reader Loop, TL – Tag Loop).

III. Reader Side

A. Communication Part

A centre-excised Archimedes spiral antenna is designed as a dual transmitting/receiving antenna for the RFID reader and is used for communication with the RFID chip, see Fig. 3. From this point of view the antenna properties have to be optimized for working in close proximity to the human body that is represented in the design and measurement by an agar phantom, as can be seen in Fig. 1.

To verify the properties of the proposed structure of the reader side, the reader antenna matched to 50 Ω was first simulated by an IE3D method of moments simulator on a human body agar phantom ($110 \times 80 \times 15$ mm^3, $\varepsilon_r \sim 55$, tan(δ) ~ 0.5), according to Fig. 1. A comparison of the simulated and measured reflection coefficients and gains of the reader antenna on the human body agar phantom, according to Fig. 1, is presented in Fig. 5 and in Table I. A highly satisfactory impedance matching at an operating frequency of 866 MHz, in addition to a satisfactory gain, can be observed. Fig. 6 shows a comparison of the simulated and measured radiation patterns in both principal planes at 866 MHz. A very successful agreement, and functional radiation pattern shape, can be observed. The radiation pattern exhibits decrease in the direction of the human body agar phantom caused by phantom absorption.

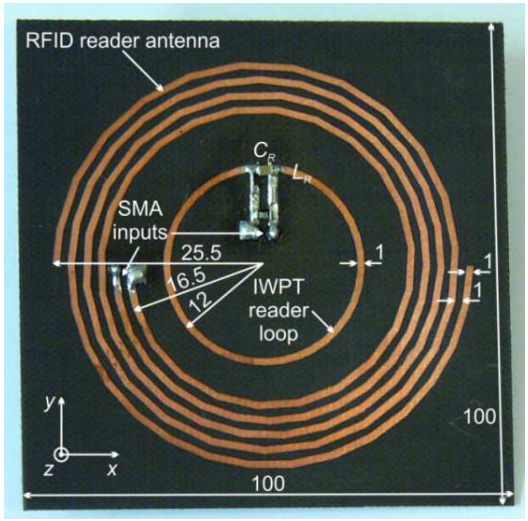

Fig. 3. Photograph of the reader side structure (dimensions in mm).

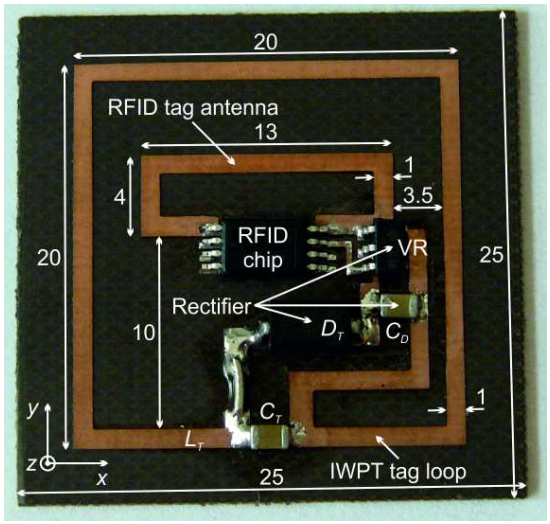

Fig. 4. Photograph of the tag side structure (dimensions in mm).

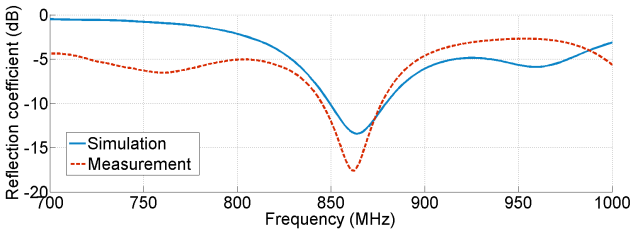

Fig. 5. Simulated and measured reflection coefficients of centre-excised Archimedes spiral RFID reader antenna situated on human body agar phantom.

TABLE I
Simulated and Measured Reflection Coefficients S_{11} and Gains G of Centre-Excised Archimedes Spiral RFID Reader Antenna Situated on the Human Body Agar Phantom at Operating Frequency of 866 MHz

	S_{11} (dB)	G (dBi)
Simulation	−13.3	−12.2
Measurement	−16.2	−11.0

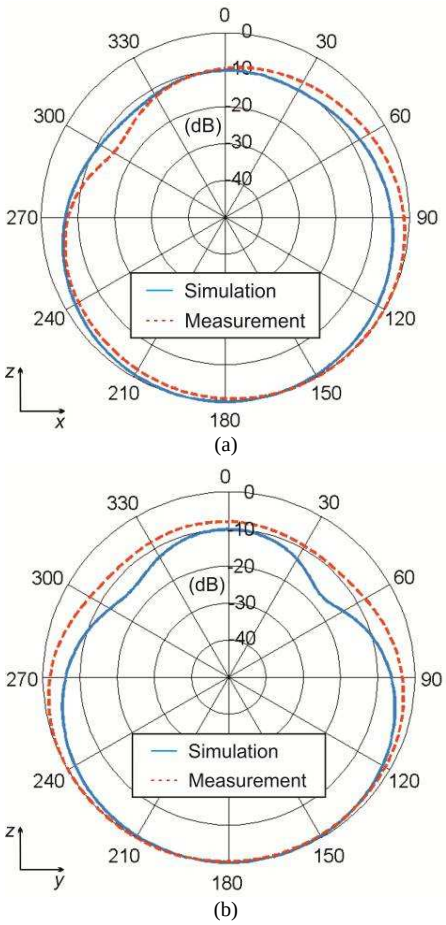

Fig. 6. Simulated and measured radiation patterns of the centre-excised Archimedes spiral RFID reader antenna situated on a human body agar phantom at operating frequency of 866 MHz. (a) *xz*-plane. (b) *yz*-plane.

B. *Powering Part*

A circular loop is used as a transmitting element for the IWPT on the reader side, as shown in Fig. 3. A simple loop is chosen due to having little influence on the reader antenna. The measured self-inductance and resistance of the reader loop have values L_R = 53.6 nH and R_R = 0.066 Ω respectively. The reactance of the reader loop is compensated by a capacitor of value C_R = 10 nF to form a parallel resonant circuit at the operating frequency of 6.78 MHz. The resonant circuit assures purely resistive input impedance as seen by the power source.

IV. Tag Side

A. *Communication Part*

A folded dipole is used as an antenna for the RFID tag, see Fig. 4. The tag antenna should operate as an implant situated inside a human body. Therefore, the antenna properties have to be optimized under these conditions. The antenna is fed by an RFID chip with complex input impedance Z_{CHIP} = 7.4 − j122 Ω at the operating frequency of 866 MHz in semi-active mode. The tag antenna matched to the chip was designed with complex input impedance Z_{ANT} = 7.4 + j122 Ω at 866 MHz. The tag antenna was manufactured and measured as a separate sample fed by an SMA connector, without the RFID chip, to verify the properties of the proposed structure.

A comparison of the simulated and measured input impedances of the tag antenna situated inside the human body agar phantom ($110 \times 80 \times 30$ mm^3, $\varepsilon_r \sim 55$, $\tan(\delta) \sim 0.5$), according to Fig. 1, is shown in Fig. 7. Fig. 8 shows simulated and measured transmission coefficients between the tag antenna situated in the agar phantom and the RFID chip in semi-active mode. Simulated and measured gains and simulated radiation patterns of the tag antenna at the operating frequency of 866 MHz can be seen in Table II and Fig. 9 respectively. The value of the gain is acceptable for this class of implantable antennas [6-8].

B. *Powering Part*

A simple, rectangular loop, with little influence on the tag antenna, is used as the receiving element for the IWPT on the tag side, as shown in Fig. 4. The measured self-inductance and resistance of the tag loop have values L_T = 55.9 nH and R_T = 0.068 Ω respectively, with the tag loop being coupled to the reader loop by mutual inductance M = 3 nH (measured value for the arrangement according to Fig. 1). A reactance of the tag loop is compensated by a capacitor of value C_T = 10 nF to form a parallel resonant circuit at the operating frequency of 6.78 MHz. The resonant circuit assures a sufficient level of voltage for the following simple rectifier which consists of a zero bias Schottky diode D_T, capacitor C_D = 10 nF, and a voltage regulator connected to the powering pins of the RFID chip.

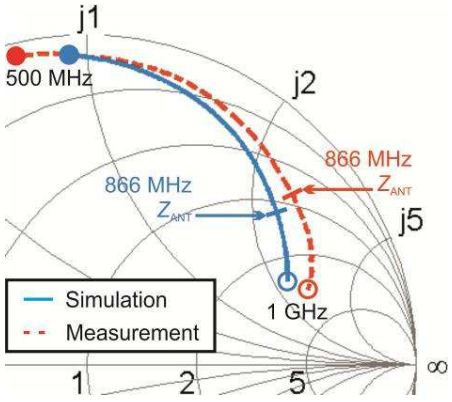

Fig. 7. Simulated and measured input impedances of folded dipole RFID tag antenna in a Smith chart in the frequency band 500 MHz – 1 GHz.

V. Measurement of System Properties

The improvement of sensitivity of the RFID chip is verified by measurements with and without powering and the minimum reader transmitted power P_{Tmin} for a constant reading distance, according to Fig. 1, is investigated, see Table III.

Operating the RFID chip in a semi-active mode, with powering by the IWPT, allows the chip to increase in sensitivity from −8.3 dBm (passive mode) to −31 dBm (semi-active mode) according to [12]. It has been verified by measurement that the minimum reader transmitted power P_{Tmin} is reduced by approximately 21 dB, from 29 dBm in the

passive mode to 8 dBm in the semi-active mode in the arrangement, according to Fig. 1. The measured reader transmitted power reduction (21 dB) corresponds satisfactorily to the increase of theoretical RFID chip sensitivity in the semi-active mode (22.7 dB). A relatively small difference (1.7 dB) is caused by chips manufacturing tolerances and by non-perfect testing in a complex environment.

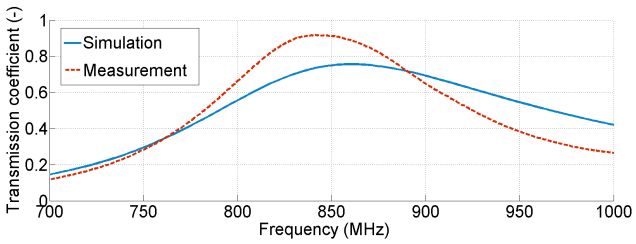

Fig. 8. Simulated and measured transmission coefficient between the folded dipole RFID tag antenna situated in a human body agar phantom and the RFID chip in semi-active mode.

TABLE II
SIMULATED AND MEASURED TRANSMISSION COEFFICIENTS τ AND GAINS G OF FOLDED DIPOLE RFID TAG ANTENNA SITUATED IN THE HUMAN BODY AGAR PHANTOM AT OPERATING FREQUENCY OF 866 MHZ

	τ (-)	G (dBi)
Simulation	0.75	−24.9
Measurement	0.87	−22.0

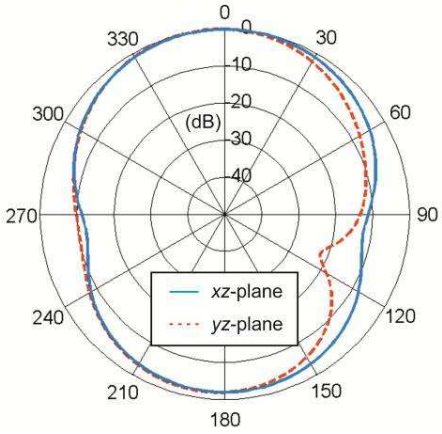

Fig. 9. Simulated radiation patterns of a folded dipole RFID tag antenna situated in a human body agar phantom at operating frequency of 866 MHz.

TABLE III
SYSTEM SENSITIVITY MEASUREMENT

Chip mode	Chip sensitivity (dBm)	P_{Tmin} (dBm)
Passive	−8.3	29
Semi-active	−31	8

VI. CONCLUSION

A compact system for an implantable battery-less semi-active UHF RFID tag was designed, fabricated, and measured. This system integrates an RFID communication part operating at frequency 866 MHz and an IWPT powering part operating at frequency 6.78 MHz. The reader side is composed of a communication centre-excised Archimedes spiral antenna located on one substrate, together with a powering circular loop. The communication on the tag side proceeds via a folded dipole antenna integrated inside a powering rectangular loop. Efficient performance of the IWPT is assured by the resonant principle and a simple rectifier with a zero bias Schottky diode.

The system is designed to operate wirelessly the tag inside human body tissue represented by an agar phantom. The experiment verified the aim of the design: the sensitivity of the communication of the RFID chip has been improved by about 21 dB when the chip is powered by the IWPT. This allows the power level of the communication signal to be reduced significantly. Exposure limits to time-varying electromagnetic field [13] are not taken into account for the powering part of the system at this moment. Optimization of the structure with respect to exposure limits is expected to be treated in the future work.

REFERENCES

[1] S. Rao, J.-C. Chiao, "Body Electric: Wireless Power Transfer for Implant Applications", *IEEE Microw. Magazine*, vol. 16, no. 2, pp. 54–64, 2015.

[2] K. Finkenzeller, "RFID Handbook: Fundamentals and Applications in Contactless Smart Cards and Identification", 2nd edition, John Wiley & Sons, 2005.

[3] J. Kracek, M. Mazanek, "Wireless Power Transmission for Power Supply: State of Art", *Radioengineering*, vol. 20, no. 2, pp. 457–463, 2011.

[4] J. H. Schulman, J. P. Mobley, J. Wolfe, E. Regev, C. Y. Perron, R. Ananth, E. Matei, A. Glukhovsky, R. Davis, "Battery powered BION FES network", in *Proc. 26th Annual International Conference of the IEEE Engineering in Medicine and Biology*, pp. 4283–4286, 2004.

[5] M. Ghovanloo, S. Atluri, "A Wide-Band Power-Efficient Inductive Wireless Link for Implantable Microelectronic Devices Using Multiple Carriers", *IEEE Transactions on Circuits and Systems I: Regular Papers*, vol. 54, no. 10, pp. 2211–2221, 2007.

[6] D. C. Sirait, Basari, F. Y. Zulkifli, E. T. Rahardjo, "An Implanted Dipole Antenna for RFID-Based Patient Monitoring System", in *Proc. Quality in Research (QiR)*, Yogyakarta, Indonesia, pp. 142–145, 2013.

[7] J. Ung, T. Karacolak, "A Wideband Implantable Antenna for Continuous Health Monitoring in the MedRadio and ISM Bands ", *IEEE Antennas Wireless Propag. Lett.*, vol. 11, pp. 1642–1645, 2012.

[8] H.-Y. Lin, M. Takahashi, K. Saito, K. Ito, "Development of UHF Implanted RFID Antenna for Medical/Health-care Applications", in *Proc. General Assembly and Scientific Symposium (URSI)*, Istanbul, Turkey, pp. 1–4, 2011.

[9] L. Vojtěch, L. Kypus, L. Kvarda, N. Thiard, J. Yannis, "Solar and Wireless Energy Harvesting Semi-Active UHF RFID Tag Design and Prototyping", in *Proc. 16th International Conference on Mechatronics (ME)*, Brno, Czech Republic, pp. 188–193, 2014.

[10] H. Chu, G. Wu, J. Chen, Y. Zhao, "Study and Simulation of Semi-Active RFID Tags Using Piezoelectric Power Supply for Mobile Process Temperature Sensing", in *Proc. IEEE International Conference on Cyber Technology in Automation, Control, and Intelligent Systems*, Kunming, China, pp. 38–42, 2011.

[11] XR 480 specifications. (2012). Datasheet. [Online]. Available: http://www.symbol.com.

[12] EM 4325 specifications. (2015). Datasheet. [Online]. Available: http://www.emmicroelectronic.com.

[13] A. Ahlbom at al., "Guidelines for limiting exposure to time-varying electric, magnetic, and electromagnetic fields (up to 300 GHz)", *Health Physics*, vol. 74, no. 4, pp. 494–521, 1998.